PERGAMON

International Journal of Solids and Structures 40 (2003) 4239–4256

INTERNATIONAL JOURNAL OF SOLIDS and STRUCTURES

www.elsevier.com/locate/ijsolstr

Damping in ceramic matrix composites with matrix cracks

Victor Birman [a,*], Larry W. Byrd [b]

[a] Engineering Education Center, University of Missouri-Rolla, 8001 Natural Bridge Road, St. Louis, MO 63121, USA
[b] Air Force Research Laboratory, AFRL/VASM, Building 65, 2790 D Street, Wright-Patterson Air Force Base, OH 45433, USA

Received 12 March 2003; received in revised form 12 March 2003

Abstract

The paper presents an analytical solution capable of predicting the effect of matrix cracking in ceramic matrix composites (CMC) on damping. The cracking scenarios considered in the paper include through-the-thickness cracks and cracks terminating at the layer interfaces. The increase in damping associated with matrix cracking is mostly due to the frictional energy dissipation along the damaged fiber–matrix interfaces adjacent to the bridging cracks whose plane of propagation intersects the fiber axis. Damping increases with a higher density of matrix cracks. The loss factor is affected by the angle of the lamina relative to the direction of the applied load. The loss factor is also influenced by the frequency and magnitude of local dynamic stresses. Examples of distributions of the local loss factor along the axis of a CMC beam subject to pulsating loads of various frequencies are shown in the paper.

Keywords: Ceramic matrix composites; Damping; Cracks

1. Introduction

The purpose of the present paper is to elucidate the effect of matrix cracking in angle-ply ceramic matrix composites (CMC) on the loss factor (damping) in these materials. Two cracking scenarios are considered, including through-the-thickness cracks and the cracks limited to single layers and terminating at the layer interface. In addition, the effects of the vibration frequency and the amplitude of local stresses on damping are illustrated on the example of a CMC cantilever beam subject to axial fatigue loading.

As suggested by Wu and Erdogan (1993), cracks in composite laminates can grow within the layer until they reach the interface. Subsequently, three possibilities have to be considered. The crack may be arrested, in which case additional cracks that appear in other layers of the laminate are not necessarily collinear with the former crack. The second option is delamination cracking that originates at the interface from the tip of the initial crack. Finally, the crack may continue to grow throughout the thickness of the laminate, without changing its orientation.

* Corresponding author. Tel.: +1-314-516-5436; fax: +1-314-516-5434.
E-mail address: vbirman@umr.edu (V. Birman).

0020-7683/03/$ - see front matter © 2003 Elsevier Science Ltd. All rights reserved.
doi:10.1016/S0020-7683(03)00199-9

Nomenclature

σ	applied stress acting in the x-direction (Eq. (3))
σ_1	stress acting in the 1-direction (Eq. (3))
σ_2	stress acting in the 2-direction (Eq. (3))
τ_{12}	in-plane shear stress in the 1–2 coordinate axes (Eq. (3))
$\Delta\sigma_1$	range of tensile stresses in the 1-direction (Eq. (6))
τ	interfacial shear stress (Eq. (6))
σ_{eq}	stress acting in the 1-direction (Eq. (12))
σ_1^0	stress acting in the 1-direction in longitudinal layers (Eq. (18))
σ_x^θ	stress acting in the x-direction on the layer with the lamination angle (Eq. (18))
$\Delta\sigma$	range of applied tensile stresses (Eq. (22))
$\Delta\sigma_1^0$	range of tensile stresses acting in the x-direction in longitudinal layers (Eq. (22))
$\Delta\sigma_x^\theta$	range of tensile stresses acting in the x-direction in inclined layers (Eq. (22))
σ_{1a}^0	amplitude of tensile stresses acting in the 1-direction in longitudinal layers (Eq. (25))
σ_1'	maximum per-cycle stress in the x-direction in longitudinal layers (Eq. (26))
σ_1^x	maximum per-cycle stress in the x-direction in inclined layers (Eq. (26))
σ_x	amplitude of dynamic stress applied to the beam (Eq. (29))
$\Delta\sigma_i$	range of dynamic stress acting in the ith layer of the beam (Eq. (32))
σ_0	static stress applied to the beam (Eq. (33))
σ_i^0	static stress acting in the ith layer of the beam (Eq. (33))
$\sigma(x,\omega)$	local stress in the beam dependent on the location and frequency of motion (Eq. (37))
$\Delta\sigma(x,\omega)$	range of local stress in the beam (Eq. (38))

In angle-ply CMC considered here the mode of cracking is determined by the laminate construction. In particular, in balanced symmetric $[-\theta/\theta]_k$ laminates cracks may originate along one of the material symmetry planes (see Fig. 1 that introduces coordinate systems employed in the subsequent analysis). If these cracks are parallel to the fibers, they are called tunneling cracks, while the bridging cracks are perpendicular or inclined relative to the fibers. In any case, the cracks almost immediately propagate through the thickness of the corresponding layer.

In the case of $[-\theta_m/0_n/\theta_m]_k$ laminates, initial cracks may originate either in the longitudinal (0) layers as bridging cracks or in the inclined (θ) layers as tunneling cracks (Byrd and Birman, 2002). While the former case is likely to lead to through the thickness cracking, the latter case may result in the saturation of the cracks in the inclined layers followed by bridging cracking in the longitudinal layers or delamination. Based on the observation for cross-ply CMC, it can be predicted that if tunneling cracks form first, they will reach

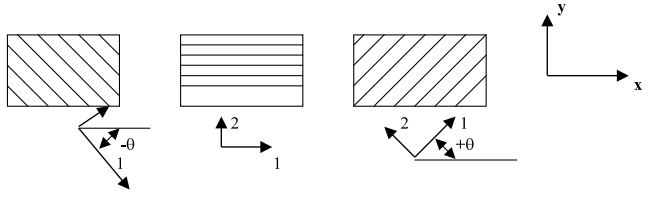

Fig. 1. Specially and generally orthotropic laminae and the coordinate systems used in the analysis.

saturation in the inclined layers, prior to propagating into the longitudinal layers (Karandikar and Chou, 1993; Domergue et al., 1996).

The present paper deals with damping in $[-\theta/\theta]_k$ and $[-\theta_m/0_n/\theta_m]_k$ laminates. The approach to the evaluation of the increase in damping due to damage is suggested for the case of bridging matrix cracking. The change in damping in the case of tunneling cracks was shown to be limited (Birman and Byrd, 2002) and it is not analyzed here. It is worth mentioning here surveys dealing with damping in composite materials that have been published by Bert (1980, 1991); Adams (1987) and Gibson (1992). However, it should be noted that an analytical prediction of damping in damaged composite materials has not been thoroughly investigated.

In addition to the general solution, the results obtained in the paper were used to predict the loss factor of a CMC beam with bridging matrix cracks as a function of the local stresses. These stresses are affected by the magnitude and frequency of the externally applied load. Therefore, both these parameters influence the value of the local loss factor that varies along the beam axis. This phenomenon is illustrated on the example of a CMC cantilevered beam subject to axial dynamic loading.

2. Analysis

2.1. Estimate of damping in a generally orthotropic lamina with bridging matrix cracks

Damping can be expressed in terms of the loss factor that is defined by

$$g = \frac{U_{\mathrm{d}}}{2\pi U} \tag{1}$$

where U_{d} is the density of energy dissipated during the cycle of motion, while U is the maximum strain energy density per cycle. If the structure includes several linear viscoelastic elements, the previous equation can be modified as suggested by Ungar and Kerwin (1962):

$$g = \frac{\sum_i g_i W_i}{\sum_i W_i} \tag{2}$$

where W_i is the maximum strain energy in the ith element during the cycle, and g_i is the loss factor of the corresponding element.

The analysis of damping can be performed for either bridging or tunneling matrix cracks in the layers. The loss factor of the $[-\theta/\theta]_k$ laminate is equal to the loss factor of individual layers if the same crack density is anticipated in all layers (this occurs if the load that caused cracking was uniformly distributed through the thickness of the laminate). Based on the previous analysis (Birman and Byrd, 2002), it can be predicted that the changes in damping in the case of tunneling cracking will be small. Accordingly, considering the fact that the loss factors of intact ceramics and CMC are very small (Pant and Gibson, 1996; Yang et al., 1997; Lee, 1966), it is possible to assume that tunneling cracking will result in an insignificant increase in damping. The situation is different if bridging matrix cracks develop in the layers. In this case, the increase in damping is very considerable and it is mostly related to the interfacial fiber–matrix friction along the slip regions adjacent to the plane of the crack. Therefore, the subject of the following discussion is damping in an angle-ply lamina with bridging matrix cracks.

If a balanced symmetrically laminated CMC panel is subject to axial stresses σ (for clarity, notation for stresses is presented in nomenclature), the stresses in the principal material coordinate system 1–2 can be calculated by the transformation equations:

$$\begin{aligned}\sigma_1 &= \sigma\cos^2\theta\\ \sigma_2 &= \sigma\sin^2\theta\\ \tau_{12} &= \sigma\cos\theta\sin\theta\end{aligned} \tag{3}$$

Subsequently, the strains in the principal material directions are available from

$$\begin{aligned}\varepsilon_1 &= a_{11}\sigma_1 + a_{12}\sigma_2\\ \varepsilon_2 &= a_{12}\sigma_1 + a_{22}\sigma_2\\ \gamma_{12} &= a_{66}\tau_{12}\end{aligned} \tag{4}$$

where the compliance coefficients expressed in terms of the engineering constants of an orthotropic layer (standard notation) are:

$$\begin{aligned}a_{11} &= 1/E_1\\ a_{12} &= -v_{12}/E_1\\ a_{22} &= 1/E_2\\ a_{66} &= 1/G_{12}\end{aligned} \tag{5}$$

During the tensile part of the fatigue loading cycle, the stiffness of the layers with bridging cracks varies, reflecting sliding of the fibers along the matrix (partial or full slip). Therefore, it is necessary to specify the values of engineering constants in (5). This can be done following the approach suggested by Birman and Byrd (2001). First, the average modulus of elasticity for the tensile part of the cycle is calculated following the solution of Sorensen and Holmes (1996):

$$\begin{aligned}E_1 &= \frac{\tau}{\frac{\tau}{E_L} + \frac{r}{4s}\frac{\Delta\sigma_1}{E_f}\left(\frac{V_m E_m}{V_f E_L}\right)^2}\\ E_1 &= \frac{V_f E_f}{1 - V_f\frac{s\tau}{r\Delta\sigma_1}}\end{aligned} \tag{6}$$

where the first equation corresponds to a partial fiber–matrix slip, while the second equation should be used in the case of a full fiber–matrix slip.

In (6), τ is the interfacial shear stress, r is the fiber radius, s is the preexisting bridging matrix crack spacing, $\Delta\sigma_1$ is the range of tensile stresses acting in the fiber (1) direction and E_L is the longitudinal modulus of the intact layer. The modulus and the volume fraction of the fibers are denoted by E_f and V_f, respectively. The corresponding constants of the matrix are E_m and V_m. Note that it is necessary to operate with the average per-cycle modulus of elasticity, rather than the instantaneous values, since in the latter case reduced stiffnesses depend on time and the analysis is very complicated. The boundary between the partial and full slip is defined as a function of the average per-cycle modulus. The former case occurs if

$$E_1 > \frac{V_f E_f}{1 - \frac{V_m}{2}\frac{E_m}{E_L}}$$

while the full slip corresponds to smaller values of the modulus. The range of tensile stresses $\Delta\sigma_1$ that appears in (6) can easily be evaluated from the first equation (3), provided the range of applied stresses σ acting in the x-direction is prescribed.

Now, following Birman and Byrd (2001), it is assumed that the stiffness of the lamina in the 2-direction remains unaffected by bridging matrix cracks that are perpendicular to the fibers since the crack opening (width) is negligible compared to the crack spacing. Due to the same assumption, the ratio of the applied strain in the 1-direction to the resulting strain in the 2-direction can be considered unaffected by cracks.

These considerations imply that the modulus E_2 and Poisson ratio v_{12} can be taken equal to those for the intact material, i.e. $E_2 = E_T$ and $v_{12} = v_{LT}$. Accordingly, the second in-plane Poisson ratio can be calculated as:

$$v_{21} = v_{LT}\frac{E_T}{E_1} \tag{7}$$

In addition, the in-plane shear modulus can be calculated from (Birman and Byrd, 2001)

$$G_{12} = \frac{2G_{LT}}{1 + E_L/E_1} \tag{8}$$

Now it is possible to calculate the coefficients a_{ij} given by (5) that account for the presence of bridging matrix cracks in the lamina. Note that these coefficients refer only to the tensile part of the motion cycle when the cracks are open. Under compression, the cracks are assumed closed and $E_1 = E_L$. If bridging cracks are not perpendicular to the fibers, the present approach to the evaluation of the compliance coefficients may be inaccurate and a_{ij} have to be determined from the finite element analysis.

The frictional energy dissipation density per second in the case where the stress ratio during a fatigue cycle $R = \sigma_{min}/\sigma_{max} \geqslant 0$ was derived by Cho et al. (1991):

$$W_{fric,t} = \frac{fr(\Delta\sigma_1)^3}{12sE_f\tau}\left(\frac{V_m E_m}{V_f E_L}\right)^2 \tag{9}$$

where f is a vibration frequency. Eq. (9) and the subsequent solution correspond to the case of a partial slip. The corresponding solution for a full slip can be based on the counterpart of (9) available from the paper of Sorensen and Holmes (1996). This solution is omitted here for brevity.

The density of the energy dissipated per cycle as a result on the interfacial friction can be evaluated by dividing the expression in (9) by the frequency and substituting the appropriate range of stresses. For example, if the applied stress ratio is equal to zero, as is the case if $\sigma(x) = \sigma(1 + \sin\omega t)$, the range of stresses in the fiber direction (1-direction) in the inclined layers is

$$\Delta\sigma_1 = 2\sigma_1 = 2\sigma\cos^2\theta \tag{10}$$

Accordingly, the density of energy dissipated per cycle becomes

$$U_d(\sigma_1) = \frac{2r(\sigma\cos^2\theta)^3}{3sE_f\tau}\left(\frac{V_m E_m}{V_f E_L}\right)^2 \tag{11}$$

It is assumed that the stress component σ_2 acting perpendicular to the fibers, in the plane of the cracks, does not affect the interfacial friction. However, the in-plane shear stress along the damaged section of the interface changes a relative displacement between the fiber and matrix resulting in additional interfacial friction. While the exact solution of this problem is outside the scope of the paper, an estimate of the effect of shear stresses can be obtained by introducing an equivalent axial stress acting in the fiber direction. The magnitude of this stress can be obtained from the requirement that the strain energy release rate associated with the equivalent stress should equal that rate for the actual stress state. The substitution of these energy release rates expressed in terms of the stress intensity factors according to (Kanninen and Popelar, 1985) into the above-mentioned requirement yields

$$E'\lfloor K_I^2(\sigma_1) + K_{II}^2(\tau_{12})\rfloor = E'K_I^2(\sigma_{eq}) \tag{12}$$

where E' is the plain strain modulus and the stress intensity factors are given by $\{K_I(\sigma), K_{II}(\tau)\} = \{\sigma, \tau\}\sqrt{\pi a}$, a being a half-length of the crack. Note that (12) involves the modulus affected by the range of axial stresses. However, an estimate of the effect of in-plane shear stress can be obtained by assumption that a difference in the moduli in the left and right sides of (12) is negligible. Accordingly,

$$\sigma_{\mathrm{eq}} = \sigma_1 \sqrt{1 + \left(\frac{\tau_{12}}{\sigma_1}\right)^2} \tag{13}$$

Now the density of the interfacial energy dissipation (11) can be modified to incorporate the effect of the shear stress:

$$U_{\mathrm{d}}(\sigma_1, \tau_{12}) = \frac{2r(K\sigma\cos^2\theta)^3}{3sE_{\mathrm{f}}\tau}\left(\frac{V_{\mathrm{m}}E_{\mathrm{m}}}{V_{\mathrm{f}}E_{\mathrm{L}}}\right)^2 \tag{14}$$

where

$$K = \sqrt{1 + \tan^2\theta} \tag{15}$$

The solution given by (13) and (14) can be recommended only if the shear stress and its effect are relatively small. As follows from the previous research (Byrd and Birman, 2002), loading applied at angles larger than 45° produces tunneling, rather than bridging, cracks. Therefore, the present analysis can be recommended if both the initial load that caused damage and the subsequent fatigue loads are oriented at an angle equal or smaller than 45° relative to the fiber direction.

The maximum strain energy density is available from

$$U = \frac{1}{2}\left(\frac{\sigma_{1\mathrm{m}}^2}{E_1} + \frac{\sigma_{2\mathrm{m}}^2}{E_2} + \frac{\tau_{12\mathrm{m}}^2}{G_{12}}\right) = \frac{\sigma_{\max}^2}{2E_x} \tag{16}$$

where $\{\sigma_{1\mathrm{m}}, \sigma_{2\mathrm{m}}, \tau_{12\mathrm{m}}\}$ represent the combination of simultaneously applied stresses in the 1–2 coordinate system that result in the maximum strain energy density during the cycle of motion, $E_1 = E_1(\sigma_1)$, $G_{12} = G_{12}(\sigma_1)$, $E_2 = E_{\mathrm{T}}$ (strictly speaking, this is correct only if the cracks are perpendicular to the fibers), and $\sigma_{\max}$ is the maximum tensile stress during the cycle acting in the x-direction. The modulus of the lamina in the x-direction, E_x, can easily be evaluated as a function of the moduli in the lamina principal directions. Obviously, this modulus is a function of the range of tensile stresses.

The loss factor calculated by assumption that the only source of increased damping is the interfacial friction can be now evaluated. Note that this conservative approach is based on the assumed negligible changes in damping due to reduced stiffness associated with damage, local stress concentrations at the tips of the cracks, thermomechanical coupling, etc. Accordingly, the loss factor of a layer that coincides in the case of $[-\theta/\theta]_k$ laminates subject to uniform through the thickness loads with the loss factor of the laminate is given by

$$g' = g + \frac{U_{\mathrm{d}}(\sigma_1, \tau_{12})}{2\pi U} \tag{17}$$

where g is the loss factor of the intact lamina calculated as explained in Appendix A, U is given by (16), and U_{d} is substituted from (14).

2.2. Damping in $[-\theta_m/0_n/\theta_m]_k$ angle-ply CMC

This type of angle-ply laminates is often used in industry because of enhanced stiffness in the x-direction. The initial mode of damage in such laminates is in the form of bridging cracks in the longitudinal layers or tunneling cracks in the inclined layers. As was shown by Byrd and Birman (2002), bridging cracks in the inclined layers are unlikely to constitute the initial mode of damage.

Two cases considered in the present study include damping in CMC laminates with bridging cracks in longitudinal layers and tunneling cracks in inclined layers and damping in laminates with through-the-

thickness matrix cracks originating in longitudinal layers. The former case is anticipated if initial cracking occurred in inclined layers, while the latter case can occur if cracks originated in longitudinal layers.

2.2.1. Damping in angle-ply $[-\theta_m/0_n/\theta_m]_k$ laminates with tunneling cracks in transverse layers and bridging cracks in longitudinal layers

While tunneling cracks reduce the stiffness of the transverse layers, it has been found that this change does not result in a significant increase in damping (Birman and Byrd, 2002). Accordingly, the only noticeable effect of the cracks in inclined layers on damping of the laminate can be attributed to a redistribution of the laminate stiffness and the effect on the stresses in the longitudinal layers. If a balanced $[-\theta_m/0_n/\theta_m]_k$ laminate is subject to uniaxial loading, the applied stress σ acting in the x-direction can be related to the stresses in the layers by the following approach.

The static equilibrium dictates that

$$\sigma = H_n\sigma_1^0 + H_m\sigma_x^\theta \tag{18}$$

where $H_n = n/(2m+n)$ and $H_m = 2m/(2m+n)$ are the relative thicknesses of the longitudinal and inclined layers. The stresses acting in the x-direction in the longitudinal and inclined layers are denoted by σ_1^0 and σ_x^θ, respectively. Note that the stress σ_1^0 is acting in the principal material direction of the corresponding layer.

The axial strains in the x-direction are assumed equal in all layers as is the case where the load is uniform through the thickness of the laminate:

$$\frac{\sigma}{E_x} = \frac{\sigma_1^0}{E_1} = \frac{\sigma_x^\theta}{E_x^\theta} \tag{19}$$

where the Poisson effect is neglected (otherwise, we have to employ the corresponding reduced stiffnesses), and E_x, E_1 and E_x^θ denote the stiffness of the laminate in the x-direction, the stiffness of longitudinal layers in the 1-direction (as in the previous section), and the stiffness of the inclined layers in the x-direction, respectively.

The engineering constants of the inclined layers can be determined following the approach suggested by Han and Hahn (1989) for the stiffness evaluation in a cross-ply material with tunneling cracks in the transverse layers. According to experimental observations (Karandikar and Chou, 1993; Domergue et al., 1996), tunneling cracks reach saturation in the transverse layers, prior to penetrating into adjacent layers (in our case, into longitudinal layers). In the present investigation, we consider the case where the cracks first developed in the inclined layers and the bridging cracks in the longitudinal layers appeared only at a later phase of loading. Therefore, it is possible to adopt the solution of Han and Hahn (1989) for the analysis of a laminate with tunneling cracks in transverse layers and intact longitudinal layers. In this case, it is possible to use the properties of the intact longitudinal layers in the principal material directions of the inclined layers. The fact that the longitudinal layers are not perpendicular to the inclined layers does not alter the analysis. Hence, if the tunneling crack spacing in the inclined layers is prescribed, one can evaluate the engineering constants of the laminate in the principal material directions of the inclined layers, namely, $E_1^{\theta\text{lam}}$, $E_2^{\theta\text{lam}}$, $\nu_{12}^{\theta\text{lam}}$, $\nu_{21}^{\theta\text{lam}}$, $G_{12}^{\theta\text{lam}}$. In these notations, "lam" indicates that the corresponding engineering constants are calculated for the composite material, including both longitudinal and inclined layers, while θ implies that the coordinate system refers to the principal material directions of the inclined layers. Note that the stiffness in the fiber direction of the inclined layers is not affected by tunneling cracks. Therefore, $E_1^{\theta\text{lam}}$ and $\nu_{21}^{\theta\text{lam}}$ correspond to the values for the intact material. Accordingly, instead of using the approach employed by Han and Hahn (1989) for the calculation of the Poisson ratio $\nu_{12}^{\theta\text{lam}}$, it is easier to calculate $\nu_{12}^{\theta\text{lam}} = \nu_{21}^{\theta\text{lam}} E_1^{\theta\text{lam}}/E_2^{\theta\text{lam}}$.

The engineering constants of the inclined layers with tunneling cracks can now be found from the static equilibrium equations. For example, the equilibrium of stresses in the 2-direction of the inclined layers yields

$$\sigma_2^\theta = E_2^{\theta\text{lam}}\varepsilon_2^\theta = H_n E_2^{\theta\text{long}}\varepsilon_2^\theta + H_m E_2^{\theta\text{incl}}\varepsilon_2^\theta \tag{20}$$

where "long" and "incl" stand for the longitudinal and inclined layers, respectively. Canceling the strain in (20) and using the known value of the stiffness for intact longitudinal layers, $E_2^{\theta\text{long}}$, yields the value of $E_2^{\theta\text{incl}}$. The shear modulus of the inclined layers can be obtained in a similar manner by considering in-plane shear stresses. Subsequently, the Poisson ratio for the inclined layers is available from

$$\nu_{12}^{\theta\text{incl}} = \nu_{21}^{\theta\text{incl}} \frac{E_1^{\theta\text{incl}}}{E_2^{\theta\text{incl}}} \tag{21}$$

where the terms in the numerator in the right side correspond to the values available for the intact material.

Now it is possible to consider the stresses and the stiffness of the longitudinal layers with bridging matrix cracks. The modulus of elasticity in the x-direction (1-direction for the longitudinal layers) and the Poisson ratio affected by bridging cracks are available from (6) and (7). However, it is necessary to specify the range of the stresses in the longitudinal layers. This can be done using (18) and (19) to evaluate σ_1^0. The modulus E_x^θ in (19) can be evaluated using the engineering constants for cracked inclined layers. Therefore, the problem of the evaluation of the stress in the longitudinal layers can be formulated as (partial fiber–matrix slip)

$$\Delta\sigma = H_n \Delta\sigma_1^0 + H_m \Delta\sigma_x^\theta \tag{22}$$

$$\Delta\sigma_1^0 \left[\frac{1}{E_\text{L}} + \frac{r}{4s\tau} \frac{\Delta\sigma_1^0}{E_\text{f}} \left(\frac{V_\text{m} E_\text{m}}{V_\text{f} E_\text{L}} \right)^2 \right] = \frac{\Delta\sigma_x^\theta}{E_x^\theta} \tag{23}$$

where $\Delta\sigma$ is the range of the applied tensile stresses, and $\Delta\sigma_1^0$ and $\Delta\sigma_x^\theta$ are the ranges of tensile stresses for the longitudinal and inclined layers in the x-direction, respectively.

Given the bridging matrix crack spacing and the interfacial shear stress, the stress range in the longitudinal layers $\Delta\sigma_1^0$ can be calculated from (22) and (23) as a function of the applied stress range $\Delta\sigma$. The stress range $\Delta\sigma_x^\theta$ is also evaluated from this set of equations.

The loss factor in the laminate is now available from the counterpart of (17):

$$g'' = g_\text{lam} + \frac{U_\text{dlong}}{2\pi U_\text{lam}} \tag{24}$$

In (24), g_lam is the loss factor for the intact laminate. The energy dissipation density associated with the interfacial friction in the longitudinal layers is shown below for a positive stress ratio R by assumption of partial slip along the fiber–matrix interface:

$$U_\text{dlong} = \frac{2r(\sigma_{1\text{a}}^0)^3}{3s\tau E_\text{f}} \left(\frac{V_\text{m} E_\text{m}}{V_\text{f} E_\text{L}} \right)^2 \frac{n}{2m+n} \tag{25}$$

where the stress $\sigma_{1\text{a}}^0$ is the amplitude of the tensile stress acting in these layers that is available from $\Delta\sigma_1^0$.

The maximum per-cycle strain energy density is

$$U_\text{lam} = \frac{1}{2} \left[\frac{(\sigma_1')^2}{E_x^0} H_n + \frac{(\sigma_x')^2}{E_x^\theta} H_m \right] \tag{26}$$

where σ_1' and σ_x' are the maximum per-cycle stresses in the x-direction acting in the longitudinal and inclined layers, respectively.

The first term in the right side of (26) reflects the strain energy density contributed by the longitudinal layers. It should be remembered that the modulus E_x^0 depends on the stress range acting in these layers, as is reflected in Eq. (6).

2.2.2. Damping in angle-ply $[-\theta_m/0_n/\theta_m]_k$ laminates with through the thickness bridging cracks

In this case, the loss factor can be obtained from the modified equation (24):

$$g''' = g_{\text{lam}} + \frac{U_{\text{dlong}} + U_{\text{dincl}}}{2\pi U_{\text{lam}}} \tag{27}$$

The density of energy dissipation in the longitudinal layers, U_{dlong}, is obtained from (25), although the maximum per-cycle stress is calculated using a different procedure outlined below. The density of energy dissipation in the inclined layers, U_{dincl}, is obtained accounting for the mixed mode of fracture, i.e. both the stresses in the fiber direction and the in-plane shear stresses.

The maximum strain energy density is available from (26). The moduli in this equation can be determined from the solution of Eq. (22) and a version of (23) where the modulus E_x^θ depends on the stresses acting in the inclined layers. The following procedure can be applied to obtain a closed-form solution.

First, one has to assume the stress range $\Delta\sigma_x^\theta$ in the inclined layers. Subsequently, the value of the average per-cycle modulus E_1^θ can be determined from (6) using the appropriate values of engineering constants. Other engineering constants of the inclined layers are immediately available using the approach outlined in the previous section and in the paper of Birman and Byrd (2001). Subsequently, the transformation equation is employed to determine the modulus E_x^θ. Now (22) and (23) contain only unknown stress ranges $\Delta\sigma$ and $\Delta\sigma_1^0$ that can be immediately determined. This accomplishes the analysis since the energy density terms in (27) can now be calculated.

3. On the effect of the vibration frequency on damping

The loss factors evaluated above are not explicitly affected by the frequency of motion. However, the frequency affects the range of stresses applied to the structure in virtually every problem. As an example, the problem of an angle-ply symmetrically laminated cantilever CMC unit-width beam subjected to an axial periodic stress $(\sigma_0 + \sigma_x \sin \omega t)$ applied at the free end is considered. It is assumed that the combination of the amplitude and frequency of the stress are such that dynamic instability does not occur. The combination of the applied static and dynamic stresses is such that the stress ratio within each layer during the cycle of motion is positive. The layers are assumed to possess bridging cracks that emerged prior to the application of the stress. In addition, it is assumed that the applied time-dependent stress does not generate additional cracks in the layers of the beam.

The equation of longitudinal vibrations of the beam is

$$A\frac{\partial^2 u}{\partial x^2} = \rho\frac{\partial^2 u}{\partial t^2} \tag{28}$$

where $A = \sum_i E_i h_i$ is the extensional stiffness obtained as a sum of the products of the dynamic modulus of elasticity in the beam axial direction and the thickness of the corresponding layer (i is the layer number), and ρ is a mass density of the material multiplied by the thickness of the beam.

The solution must satisfy the dynamic boundary conditions:

$$\begin{aligned} &u(x=0) = 0 \\ &A\frac{\partial u(x=a)}{\partial x} = \sigma_x h \sin \omega t \end{aligned} \tag{29}$$

where a is the length of the beam and h is its thickness.

The solution of this problem is

$$u = \frac{\sigma_x h c}{A\omega \cos\frac{\omega a}{c}} \sin\frac{\omega x}{c} \sin\omega t \tag{30}$$

where $c = \sqrt{A/\rho}$.

The dynamic stress component acting in the fiber direction in the ith layer of the beam can now be determined:

$$\sigma_i = \frac{E_i}{A} \frac{\cos\frac{\omega x}{c}}{\cos\frac{\omega a}{c}} \sigma_x h \sin\omega t \cos^2\theta_i \tag{31}$$

where θ_i is the angle of lamination of the layer.

Obviously, the range of the dynamic stress acting in the fiber direction in the ith layer is

$$\Delta\sigma_i = 2\frac{E_i}{A} \left| \frac{\cos\frac{\omega x}{c}}{\cos\frac{\omega a}{c}} \right| \sigma_x h \cos^2\theta_i \tag{32}$$

The dynamic stress is superimposed on the static stress in the layer acting along the fibers. This stress is given by

$$\sigma_i^0 = \sigma_0 \frac{E_i^0 h}{A} \cos^2\theta \tag{33}$$

where E_i^0 is the static modulus of the corresponding layer in the beam axial direction.

In this paper, the per-cycle stress ratio in each layer is assumed positive, $R \geqslant 0$, i.e. $\sigma_i^0 \geqslant \Delta\sigma_i/2$. Note that the analysis is performed by assumption that the fibers experience partial slip. Otherwise, the equations for the moduli and the density of energy dissipation employed below have to be modified.

The difficulty in using the solution shown above is apparent. The stresses in the layers have to be evaluated as functions of the layer moduli. However, these moduli are dependent on the stresses. Therefore, the solution has to be iterative, i.e. the initial moduli values may be assumed for the intact material, the stress values evaluated using these moduli, the moduli updated using the previously calculated stresses, etc.

Once the moduli of the layers and the stresses in these layers have been evaluated, the local density of the interfacial energy dissipation in a generally orthotropic layer is available from a modified equation (14):

$$U_{\mathrm{d}}^i = \frac{2r(K\sigma_x \cos^2\theta_i)^3}{3sE_{\mathrm{f}}\tau} \left(\frac{V_{\mathrm{m}}E_{\mathrm{m}}}{V_{\mathrm{f}}E_{\mathrm{L}}}\right)^2 \left(\frac{E_i h}{A}\right)^3 \left| \frac{\cos\frac{\omega x}{c}}{\cos\frac{\omega a}{c}} \right|^3 \tag{34}$$

Obviously, if the layer is oriented along the beam axis, $\theta = 0$ and $K = 1$.

The local loss factor that depends both on the location as well as the frequency of motion is obtained as

$$g(x,\omega) = g_{\mathrm{beam}} + \frac{\sum_i U_{\mathrm{d}}^i}{2\pi U_{\mathrm{beam}}} \tag{35}$$

where g_{beam} and U_{beam} denote the loss factor of the intact beam material and the maximum per-cycle strain energy density of the beam material, respectively. The loss factor of the intact beam material can be found as shown in Appendix A. Note that this factor is independent of the magnitude or frequency of the axial stress. It is also independent of the location along the beam. The maximum per-cycle value of the strain energy density has already been determined (Eq. (16)). It is necessary to emphasize that the moduli E_1 and G_{12} in (16) are affected by the stress range. This implies that U_{beam} obtained by (16) is a function of both the axial coordinate as well as the frequency.

The average loss factor of the beam is independent of the x-coordinate, but it is still affected by the frequency. This factor can be obtained from

$$g(\omega) = g_{\text{beam}} + \frac{\sum_i \int_0^a U_{\text{d}}^i \, \mathrm{d}x}{2\pi \int_0^a U_{\text{beam}} \, \mathrm{d}x} \tag{36}$$

A simple illustration of the effects of the frequency and coordinate on the loss factor is the case where the beam is composed of just one layer with the fibers oriented along the beam axis. In this case, the stresses acting along the beam axis are

$$\sigma(x,\omega) = \sigma_0 + \sigma_x \frac{\cos\frac{\omega x}{c}}{\cos\frac{\omega a}{c}} \sin\omega t \tag{37}$$

The range of the stresses is, of course,

$$\Delta\sigma(x,\omega) = 2\sigma_x \left| \frac{\cos\frac{\omega x}{c}}{\cos\frac{\omega a}{c}} \right| \tag{38}$$

This range can be used in (6) to evaluate a distribution of the modulus $E_1 = E(x,\omega)$. The loss factor $g_{\text{layer}}(x,\omega)$ is available from (17) using the value of the lamination angle equal to zero:

$$g_{\text{layer}}(x,\omega) = g + \frac{rE_1(\Delta\sigma)}{6\pi s E_{\text{f}}} \frac{\sigma_x}{\tau} \left| \frac{\cos\frac{\omega x}{c}}{\cos\frac{\omega a}{c}} \right|^3 \left(\frac{V_{\text{m}} E_{\text{m}}}{V_{\text{f}} E_{\text{L}}} \right)^2 \tag{39}$$

Note that the loss factor is a nonlinear function of both the dynamic stress amplitude and the frequency. Introducing a nondimensional frequency of vibrations defined as a ratio of the driving frequency to the fundamental frequency of longitudinal vibrations of the undamaged layer-beam, and a nondimensional axial coordinate, i.e.

$$\begin{aligned} w &= \frac{\omega}{\left(\frac{\pi c}{2a}\right)} \\ \bar{x} &= \frac{x}{a} \end{aligned} \tag{40}$$

the local loss factor can be represented as

$$g_{\text{layer}}(x,\omega) = g + \frac{rE_1(\Delta\sigma)}{6\pi s E_{\text{f}}} \frac{\sigma_x}{\tau} \left| \frac{\cos\frac{\pi w \bar{x}}{2}}{\cos\frac{\pi w}{2}} \right|^3 \left(\frac{V_{\text{m}} E_{\text{m}}}{V_{\text{f}} E_{\text{L}}} \right)^2 \tag{41}$$

The local modulus of elasticity in (39) and (41) is given by

$$E_1(\Delta\sigma) = \frac{\tau}{\frac{\tau}{E_{\text{L}}} + \frac{r}{2s} \frac{\sigma_x}{E_{\text{f}}} \left| \frac{\cos\frac{\pi w \bar{x}}{2}}{\cos\frac{\pi w}{2}} \right| \left(\frac{V_{\text{m}} E_{\text{m}}}{V_{\text{f}} E_{\text{L}}} \right)^2} \tag{42}$$

4. Numerical analysis

The analysis of damping is presented here for $[-\theta/\theta]_k$ angle-ply CMC laminates. Calculations were performed for a typical SiC/CAS material with the following properties (Domergue et al., 1995): $E_{\text{f}} = 200$ GPa, $E_{\text{m}} = 97$ GPa, $V_{\text{f}} = 0.35$, $r = 8 \times 10^{-6}$ m, $v_{\text{f}} = v_{\text{m}} = 0.2$ (Poisson ratios). Based on this data, $E_{\text{L}} = 133$ GPa, $E_{\text{T}} = 118$ GPa, and $G_{\text{LT}} = 50$ GPa. Two values of the bridging matrix crack spacing considered in the following examples are $s = 0.125$ mm (saturation spacing, according to experiments), and $s = 0.250$ mm. The loss factors of the fiber and matrix materials were estimated based on experimental data (Pant and Gibson, 1996; Yang et al., 1997; Lee, 1966) as $g_{\text{f}} = 0.002$, $g_{\text{m}} = 0.001$.

Based on the previous study (Byrd and Birman, 2002), it was found that the critical value of the angle of lamination is equal to 45°. In an angle-ply laminate, bridging matrix cracks develop if the lamination angle is smaller than the critical value, while tunneling cracks appear in the layers at large lamination angles. Accordingly, a sharp increase in damping attributed to a fiber–matrix friction in the case of bridging matrix cracks is observed only if $\theta < 45°$, while at larger angles the increase in damping is small and often it cannot be reliably detected. Therefore, numerical results are shown in the following figures only for the former case.

In the following examples, the interfacial shear stress was chosen equal to 5 MPa. This choice is related to the experimentally observed rapid decrease in this stress during the first fatigue cycles that is associated with a decrease in fiber roughness (Jerro et al., 1991; Rouby and Reynaud, 1993; Evans et al., 1995). It has been reported that the decrease to the threshold value occurs during the first 10–1000 cycles of motion, dependent on the material (Evans et al., 1998; Vanwijgenhoven et al., 1999). In the material considered here, the lowest measured interfacial shear stress is about 5 MPa, and accordingly, this value was used in the vibration analysis.

Variations in the loss factor of the intact lamina subject to axial loading are shown in Fig. 2. The changes in damping with the lamination angle are relatively small. Considering the order of magnitude of the loss factor, these variations are relatively insignificant in practical applications.

Both the stiffness and damping of generally orthotropic laminae with bridging matrix cracks are considered in Figs. 3–5. As follows from Fig. 3, the stiffness of a lamina subject to axial loading increases with the lamination angle. This is predictable since a larger lamination angle results in a smaller range of axial tensile stresses acting in the fiber direction. Accordingly, an average degradation of the stiffness available from Eq. (6) is less pronounced, as compared to the case where the angle of lamination is small or equal to zero. A higher density of cracks corresponds to a lower stiffness of the material. As follows from Fig. 3, a larger amplitude of the applied stress predictably results in a more significant reduction in the modulus of elasticity.

The loss factor of a generally orthotropic lamina is shown as a function of the lamination angle in Figs. 4 and 5. In these figures, the loss factor is much higher than the factor obtained for the intact lamina (Fig. 2). The results shown in Figs. 4 and 5 account for the effect of in-plane shear stresses in the lamina coordinate axes. The comparison between the loss factor evaluated neglecting these stresses and the factor accounting for them shown in Fig. 4 confirm that neglecting this effect results in a significant error that increases with the angle of lamination. As follows from the results shown in Figs. 4 and 5, the density of matrix cracks has a very significant effect on damping.

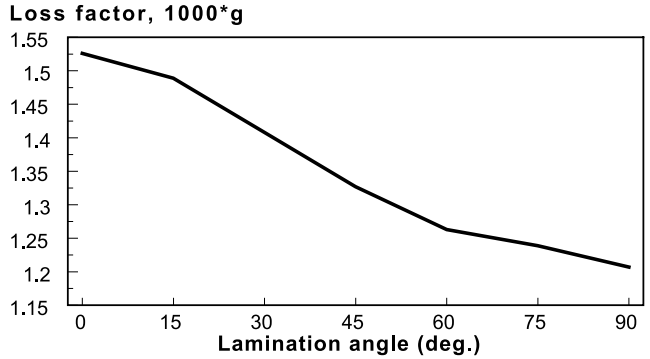

Fig. 2. Variations of the loss factor in an intact lamina subject to axial loading as a function of the lamination angle.

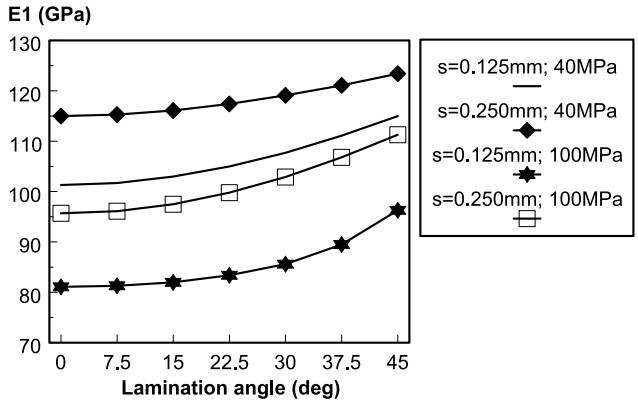

Fig. 3. Effect of the lamination angle on the longitudinal modulus in the fiber direction for a generally orthotropic lamina with bridging matrix cracks, $R = 0$, $\tau = 5$ MPa. The stress amplitudes are $\sigma = 40$ MPa and $\sigma = 100$ MPa.

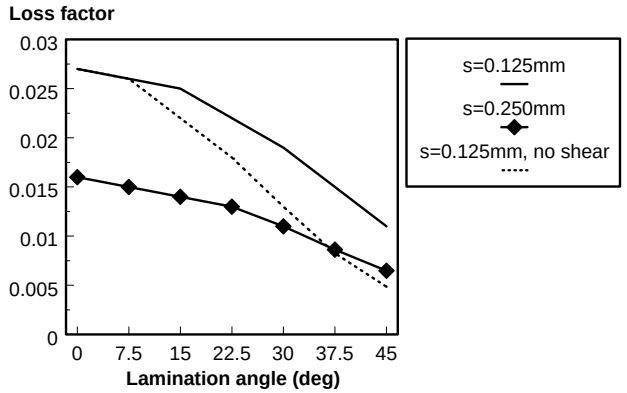

Fig. 4. Loss factor of a CMC lamina with bridging matrix cracks as a function of the lamination angle and crack spacing. The stress amplitude $\sigma = 40$ MPa, $R = 0$, $\tau = 5$ MPa.

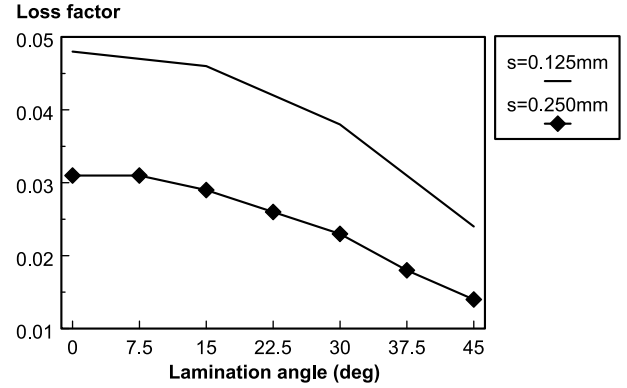

Fig. 5. Loss factor of a CMC lamina with bridging matrix cracks as a function of the lamination angle and crack spacing. The stress amplitude $\sigma = 100$ MPa, $R = 0$, $\tau = 5$ MPa.

The effects of vibration frequency and the location of the analyzed cross-section along the specially orthotropic cantilever CMC beam subject to a periodic axial loading was also considered for the same SiC/CAS material. The fibers were oriented along the beam axis. The load includes a constant component, so that the stress ratio remained positive at each point of the beam. The distributions of the per-cycle average modulus of elasticity and the stress amplitudes along the beam axis are shown in Figs. 6 and 7, respectively (ratio $x/a = 0$ corresponds to the clamped end, while $x/a = 1$ corresponds to the free end subject to dynamic loading). As follows from Fig. 6, the stiffness varies along the beam axis. At the point where the dynamic stress and strain are equal to zero corresponding to $x = 2/3$ (for $w = 3/2$), the modulus is equal to that of the intact material. However, other cross-sections of the beam are subject to tensile stresses and, accordingly, the average per-cycle modulus in these cross-sections is below the intact value. Note that in the case where the frequency of the applied load is lower than the fundamental frequency and there are no points corresponding to zero dynamic stress along the beam axis, the stiffness variations are smooth, reflecting a gradual variation of stress amplitudes between the clamped and free ends of the beam.

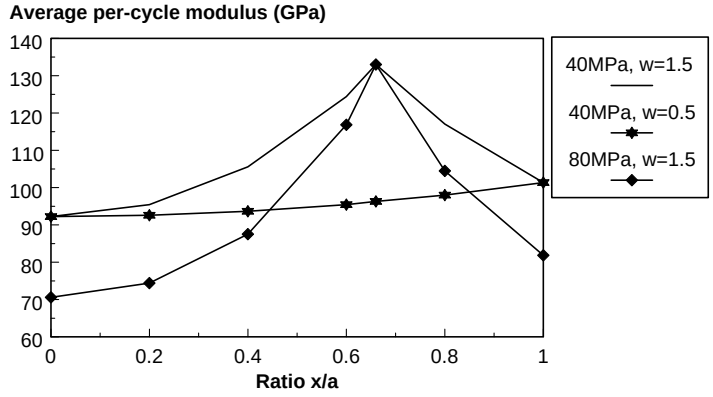

Fig. 6. Average per-cycle modulus of elasticity distribution along the axis of a specially orthotropic CMC cantilever beam subject to axial pulsating loading. Crack spacing is equal to 0.125 mm.

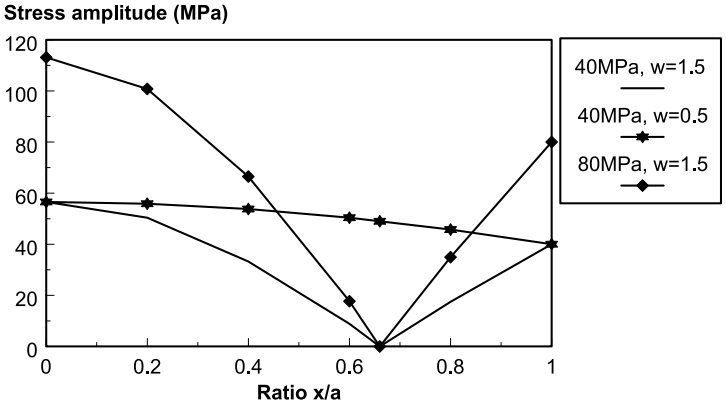

Fig. 7. Dynamic stress amplitude in a specially orthotropic CMC beam with uniform bridging matrix cracks along the axis. The beam is subject to axial pulsating loading. Crack spacing is equal to 0.125 mm.

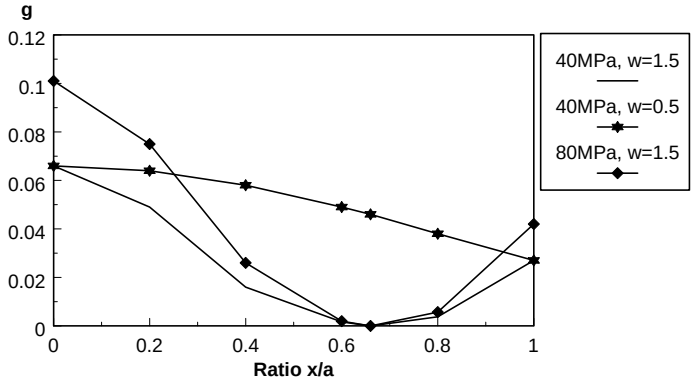

Fig. 8. Distribution of the local loss factor along the axis of a cantilever specially orthotropic CMC beam subjected to axial pulsating loading. Crack spacing is equal to 0.125 mm.

Finally, the distribution of the loss factor along the axis of the beam is illustrated in Fig. 8. It is evident from this figure, that in the presence of bridging cracks the concept of a single damping coefficient capable of characterizing the material of the structure becomes misleading. Rather, it is necessary to reflect local damping in analytical or numerical solutions. Such damping is dependent on the distribution of stresses as well as on the frequency of motion. Note that the loss factor of the material at the point where the dynamic stress is equal to zero approaches the value for the intact material that is very small (the corresponding value in Fig. 8 is so close to zero in the scale used in this figure that the impression may be created that damping "disappears" which is obviously wrong).

5. Conclusions

The study presented in this paper resulted in the following conclusions.

1. The per-cycle average longitudinal modulus of elasticity of a CMC lamina with bridging matrix cracks that is subject to tensile fatigue loading is significantly reduced compared to that of the intact lamina. This reduction becomes particularly noticeable if the cracks reach saturation.
2. The interfacial friction is responsible for an abrupt increase in damping associated with formation of bridging matrix cracks.
3. The loss factor of a generally orthotropic lamina should be evaluated accounting for the contribution of dynamic in-plane shear stresses to the slip between the fibers and matrix. This additional slip results in higher energy dissipation and a larger loss factor.
4. Higher applied dynamic stress amplitude results in a dramatic increase in damping as a result of a non-linear relationship between the tensile stress range and the loss factor.
5. The loss factor of a CMC component with bridging matrix cracks is affected by the frequency of motion and by the location. The latter effect is due to the stresses being the functions of coordinates.

Acknowledgement

This research has been supported by the Air Force Office of Scientific Research through the contract F49620-93-C-0063.

Appendix A. The loss factors of a generally orthotropic intact CMC lamina an angle-ply intact CMC laminate

The loss factor is obtained here for a generally orthotropic lamina subjected to a combination of axial and in-plane shear stresses acting in the principal material directions.

The fiber and matrix strain energy densities due to the stress σ_1 are:

$$\begin{aligned} U'_{\mathrm{f}} &= \tfrac{1}{2}V_{\mathrm{f}}\sigma_{1\mathrm{f}}\varepsilon_1 = \tfrac{1}{2}V_{\mathrm{f}}E_{\mathrm{f}}\varepsilon_1^2 \\ U'_{\mathrm{m}} &= \tfrac{1}{2}V_{\mathrm{m}}\sigma_{1\mathrm{m}}\varepsilon_1 = \tfrac{1}{2}V_{\mathrm{m}}E_{\mathrm{m}}\varepsilon_1^2 \end{aligned} \tag{A.1}$$

where the strains in the 1-direction in the fibers and matrix are equal.

The fiber and matrix strain energy densities due to the stress σ_2 are:

$$\begin{aligned} U''_{\mathrm{f}} &= \frac{1}{2}V_{\mathrm{f}}\sigma_{2\mathrm{f}}\varepsilon_{2\mathrm{f}} = \frac{1}{2}V_{\mathrm{f}}E_{\mathrm{f}2}\varepsilon_{2\mathrm{f}}^2 \\ U''_{\mathrm{m}} &= \frac{1}{2}V_{\mathrm{m}}\sigma_{2\mathrm{m}}\varepsilon_{2\mathrm{m}} = \frac{1}{2}V_{\mathrm{m}}E_{\mathrm{m}}\varepsilon_{2\mathrm{m}}^2 \end{aligned} \tag{A.2}$$

where $E_{\mathrm{f}2}$ is a transverse modulus of the fiber material that is assumed here equal to the modulus in the 1-direction (isotropic fibers).

According to the energy approach employed by Gibson (1994), the transverse strains in the fibers and in the matrix can be found as

$$\begin{aligned} \varepsilon_{2\mathrm{f}} &= a_2\varepsilon_2 \\ \varepsilon_{2\mathrm{m}} &= b_2\varepsilon_2 \end{aligned} \tag{A.3}$$

where the composite strain is $\varepsilon_2 = \sigma_2/E_{\mathrm{T}}$, i.e. a ratio of the transverse stress in the layer to its transverse modulus of elasticity. The values of coefficients in (A.3) can be found from

$$\begin{aligned} a_2V_{\mathrm{f}} + b_2V_{\mathrm{m}} &= 1 \\ E_{\mathrm{T}} &= a_2^2E_{\mathrm{f}2}V_{\mathrm{f}} + b_2^2E_{\mathrm{m}}V_{\mathrm{m}} \end{aligned} \tag{A.4}$$

The fiber and matrix strain energy densities due to the stress τ_{12} are:

$$\begin{aligned} U^{\tau}_{\mathrm{f}} &= \tfrac{1}{2}V_{\mathrm{f}}\tau_{12\mathrm{f}}\gamma_{12\mathrm{f}} = \tfrac{1}{2}V_{\mathrm{f}}G_{\mathrm{f}}\gamma_{12\mathrm{f}}^2 \\ U^{\tau}_{\mathrm{m}} &= \tfrac{1}{2}V_{\mathrm{m}}\tau_{12\mathrm{m}}\gamma_{12\mathrm{m}} = \tfrac{1}{2}V_{\mathrm{m}}G_{m}\gamma_{12\mathrm{m}}^2 \end{aligned} \tag{A.5}$$

where G_{f} and G_{m} are the shear moduli of the fibers and matrix.

The shear strains in the fibers and matrix are found following the method applied above to the transverse strains:

$$\begin{aligned} \gamma_{12\mathrm{f}} &= c_2\gamma_{12} \\ \gamma_{12\mathrm{m}} &= d_2\gamma_{12} \end{aligned} \tag{A.6}$$

where $\gamma_{12} = \tau_{12}/G_{12}$ and

$$\begin{aligned} c_2V_{\mathrm{f}} + d_2V_{\mathrm{m}} &= 1 \\ G_{\mathrm{LT}} &= c_2^2G_{\mathrm{f}}V_{\mathrm{f}} + d_2^2G_{\mathrm{m}}V_{\mathrm{m}} \end{aligned} \tag{A.7}$$

The total fiber and matrix strain energy densities can be calculated as

$$U_{\mathrm{f}} = \frac{V_{\mathrm{f}}}{2}[E_{\mathrm{f}}(\varepsilon_1^2 + a_2^2\varepsilon_2^2) + G_{\mathrm{f}}c_2^2\gamma_{12}^2]$$
$$U_{\mathrm{m}} = \frac{V_{\mathrm{m}}}{2}[E_{\mathrm{m}}(\varepsilon_1^2 + b_2^2\varepsilon_2^2) + G_{\mathrm{m}}d_2^2\gamma_{12}^2] \tag{A.8}$$

Now given the loss factors of the fiber and matrix materials, i.e. g_{f} and g_{m}, and using the total composite strain energy density equal to the sum of the contributions of the fibers and matrix, we obtain the loss factor of the intact generally orthotropic CMC lamina as

$$g = \frac{g_{\mathrm{f}}U_{\mathrm{f}} + g_{\mathrm{m}}U_{\mathrm{m}}}{U_{\mathrm{f}} + U_{\mathrm{m}}} \tag{A.9}$$

If an angle-ply CMC laminate subjected to applied stress σ_x consists of M layers, (A.9) should be generalized accordingly:

$$g = \frac{\sum_i g_{\mathrm{f}i}U_{\mathrm{f}i} + \sum_i g_{\mathrm{m}i}U_{\mathrm{m}i}}{\sum_i U_{\mathrm{f}i} + \sum_i U_{\mathrm{m}i}} \tag{A.10}$$

where summation is carried out over the index i that varies from 1 to M. Notably, (A.10) enables us to account for a possibility of using the layers composed of different materials. The stress applied to each layer can be expressed in terms of the applied laminate stress through the mechanics of materials approach. It is emphasized that the loss factor of an intact lamina or laminate subject to an axial stress is independent of the frequency or magnitude of the stress, if it is evaluated by this method. This is because all strains in the expressions (A.8) can be expressed in terms of the applied stress that cancels out in (A.9) or (A.10).

References

Adams, R.D., 1987. Damping properties analysis of composites. In: Engineered Materials Handbook. In: Reinhart, T.J. (Ed.). In: Composites, vol. I. ASM International, Materials Park, OH, pp. 206–217.

Bert, C.W., 1980. Composite materials: a survey of the damping capacity of fiber reinforced composites. In: Torvik, P.J. (Ed.), Damping Applications for Vibration Control, vol. AMD-38. ASME, New York, NY, pp. 53–63.

Bert, C.W., 1991. Research on dynamic behavior of composite and sandwich plates—V: part II. The Shock and Vibration Digest 23, 9–21.

Birman, V., Byrd, L.W., 2001. Selected issues of mechanics of ceramic matrix composites. Composite Structures 51, 181–190.

Birman, V., Byrd, L.W., 2002. Effect of matrix cracks on damping in unidirectional and cross-ply ceramic matrix composites. Journal of Composite Materials 36, 1859–1877.

Byrd, L.W., Birman, V., 2002. Onset of matrix cracking in angle-ply ceramic matrix composites. International Journal of Mechanical Sciences 44, 2173–2187.

Cho, C., Holmes, J.W., Barber, J.R., 1991. Estimation of interfacial shear in ceramic composites from frictional heating measurements. Journal of the American Ceramic Society 74, 2802–2808.

Domergue, J.-M., Vagaggini, E., Evans, A.G., 1995. Relationships between hysteresis measurements and the constituent properties of ceramic matrix composites. II: Experimental studies of unidirectional materials. Journal of the American Ceramic Society 78, 2721–2731.

Domergue, J.-M., Heredia, F.E., Evans, A., 1996. Hysteresis loops and the inelastic deformation of 0/90 ceramic matrix composites. Journal of the American Ceramic Society 79, 161–170.

Evans, A.G., Zok, F.W., McMeeking, R.M., 1995. Fatigue of ceramic matrix composites. Acta Metallurgica et Materialia 43, 859–875.

Evans, A.G., Zok, F.W., Mackin, T.J., 1998. The structural performance of ceramic–matrix composites. In: Cherepanov, G.P. (Ed.), Fracture, A Topical Encyclopedia of Current Knowledge. Kruger Publishing Co., Malabar, FL, pp. 766–839.

Gibson, R.F., 1992. Damping characteristics of composite materials and structures. Journal of Engineering Materials and Performance 1, 11–20.

Gibson, R.F., 1994. Principles of Composite Material Mechanics. McGraw-Hill, New York.

Han, Y.M., Hahn, H.T., 1989. Ply cracking and property degradation of symmetric balanced laminates under general in-plane loading. Composites Science and Technology 35, 377–397.

Jerro, P.D., Kerans, R.J., Parthasarathy, T.A., 1991. Theoretical analysis of the fiber pullout and pushout tests. Journal of the American Ceramic Society 74, 1585–1596.

Kanninen, M.F., Popelar, C.H., 1985. Advanced Fracture Mechanics. Oxford University Press, New York.

Karandikar, P., Chou, T.-W., 1993. Characterization and modeling of microcracking and elastic moduli changes in Nicalon–CAS composites. Composites Science and Technology 46, 253–264.

Lee, L.T., 1966. A graphical compilation of damping properties of both metallic and non-metallic materials. Technical report AFML-TR-66-169, Wright-Patterson Air Force Base, Dayton.

Pant, R.H., Gibson, R.F., 1996. Analysis and testing of dynamic micromechanical behavior of composite materials at elevated temperatures. Journal of Engineering Materials and Technology 118, 554–560.

Rouby, D., Reynaud, P., 1993. Fatigue behaviour related to interface modification during load cycling in ceramic–matrix fibre composites. Composites Science and Technology 48, 109–118.

Sorensen, B.F., Holmes, J.W., 1996. Fatigue of continuous fiber-reinforced ceramic matrix composites: review of mechanisms and models. In: Bressers, J., Remy, L. (Eds.), Fatigue Under Thermal and Mechanical Loadings. Kluwer Academic Publishers, Netherlands, pp. 487–499.

Ungar, E.E., Kerwin Jr, E.M., 1962. Loss factors of viscoelastic systems in terms of strain energy. Journal of the Acoustical Society of America 34 (2), 954–958.

Vanwijgenhoven, E., Wevers, M., van der Biest, O., 1999. Influence of the laminate lay-up on the fatigue behavior of SiC-fibre/BMAS-matrix composites. Composites, Part A: Applied Science and Manufacturing 30, 623–635.

Wu, B., Erdogan, F., 1993. Fracture mechanics of orthotropic laminated plates—I. The through crack problem. International Journal of Solids and Structures 30, 2357–2378.

Yang, S., Gibson, R.F., Crosbie, G.M., Allor, R.L., 1997. Dynamic mechanical properties of ceramics and ceramic composites at elevated temperatures. Journal of Engineering for Gas Turbines and Power 119, 15–19.